

# Domain Motions in Phosphoglycerate Kinase using Hierarchical NEIMO Molecular Dynamics Simulations

Nagarajan Vaidehi and William A. Goddard, III\*

Materials and Process Simulation Center, Beckman Institute (139-74), Division of Chemistry and Chemical Engineering, California Institute of Technology, Pasadena, California 91125

Received: June 16, 1999; In Final Form: November 17, 1999

We examined the large-scale domain motions in the glycolytic enzyme phosphoglycerate kinase (PGK) using the hierarchical Newton–Euler inverse mass operator (H–NEIMO) molecular dynamics (MD) method. NEIMO is an efficient MD method for torsion-only internal coordinate dynamics method. H–NEIMO is an extension of the NEIMO method for doing coarse grain MD in which large domains of a protein are treated as rigid clusters connected by flexible torsion angles. This allows an efficient examination of the low-frequency long time scale motions. We find that with both substrates bound (Phospho glycerate and ATP) on PGK the closed domain structure is more stable than the open domain structure. During the H–NEIMO MD the two domains of the open structure come close together while the N-terminus of helix 14 (namely, Gly-394 in the R65Q yeast structure) moves close to the ATP derivative, suggesting that it could be involved in the mechanism of phosphoryl transfer. We find that residues 175–183 in the R65Q yeast ternary complex structure are important in triggering the closure of the domains, resulting in a piston-like motion of helix 7. The domain rotation axis in the all atom Cartesian MD simulations is close to that of H–NEIMO MD. The axis of domain rotation in H–NEIMO is also in the same region as the rotation axis between two experimental crystal structures. Thus, H–NEIMO captures the long time scale motions in rather short simulation times. This demonstrates that H–NEIMO is a promising mesoscale coarse grain molecular dynamics technique to determine the low-frequency long time motions responsible for the function of proteins such as PGK.

## 1.0. Introduction

Molecular dynamics (MD) simulations are becoming increasingly valuable as an aid in designing, characterizing, and optimizing materials before experimental synthesis and characterization. Despite many successes, it is often not practical to follow the MD sufficiently long to observe the changes in conformations often important in determining the structure and properties of macromolecules. An important strategy for increasing the time scale is to eliminate the high frequency bond stretch and angle bend modes that set the time scale for the fundamental time step (generally to 1 fs). The Newton–Euler inverse mass operator (NEIMO) method<sup>1–4</sup> is an efficient approach of doing dynamics for just the low frequency internal torsional coordinates. This dramatically decreases the number of time steps required to follow the conformational transitions for two reasons. First, the time step can be 5–10 times larger because the high-frequency modes are missing. Second, the frictional terms due to the high-frequency modes are removed, allowing faster conformational transitions.

Herein we describe an extension of NEIMO to modeling on coarse scale. This hierarchical NEIMO uses a modified NEIMO algorithm in which the clusters may be large segments of a protein or polymer. To illustrate the use of H–NEIMO algorithm, we study the domain motions in the enzyme phosphoglycerate kinase (PGK). Here the major domains are treated as rigid bodies while properly allowing flexible torsional connections for all the amino acids connecting the two domains.

PGK catalyzes a key phosphoryl transfer reaction in the glycolytic pathway. Under physiological conditions, PGK

facilitates the phosphoryl transfer from ADP to ATP, thus converting 3-phosphoglycerate phosphate (3-PGP) to 3-phosphoglycerate (3-PG). PGK consists of two major domains (with ~1400 atoms in each domain) denoted as the C-domain and N-domain (see Figure 1). The substrate 3-PG binds to the N domain and ATP binds to the C domain. Most crystal structures reported for PGK<sup>5–9</sup> have the bound substrates 10 to 12 Å apart, far too large for catalysis. Recently three crystal structures have been reported<sup>10–12</sup> for the ternary complex of PGK which have the two domains in a closed conformation (one of these is a bisubstrate analog), with distances from 4.4 to 6.0 Å. In addition, the crystal structure of the ternary complex of PGK from yeast<sup>9</sup> (with mutation R65Q) shows the domains in an open conformation (~13.0 Å). The question here is how does PGK manage to bring the substrates together, react, and form products? One explanation is that the reactive complex, the 1,3-biphosphoglycerate<sup>9</sup> binds to an alternative site different from that observed in the crystal structures. Another is that the 20 amino acids connecting the two domains act as a large hinge, allowing the C and the N-domains to come together across the ~10 Å to react.<sup>13</sup>

This paper outlines the H–NEIMO algorithm and uses it to study the domain motions in PGK. Starting from the open domain crystal structure<sup>9</sup> of the yeast PGK that is a ternary complex, we carried out 100 ps of H–NEIMO simulations. This was sufficient to observe large-scale domain motions that bring the substrates together. These domain motions take the open structure observed in some crystals to the closed form observed in other crystals. This shows that the simple hinge bending

\* To whom correspondence should be addressed. E-mail: wag@wag.caltech.edu.

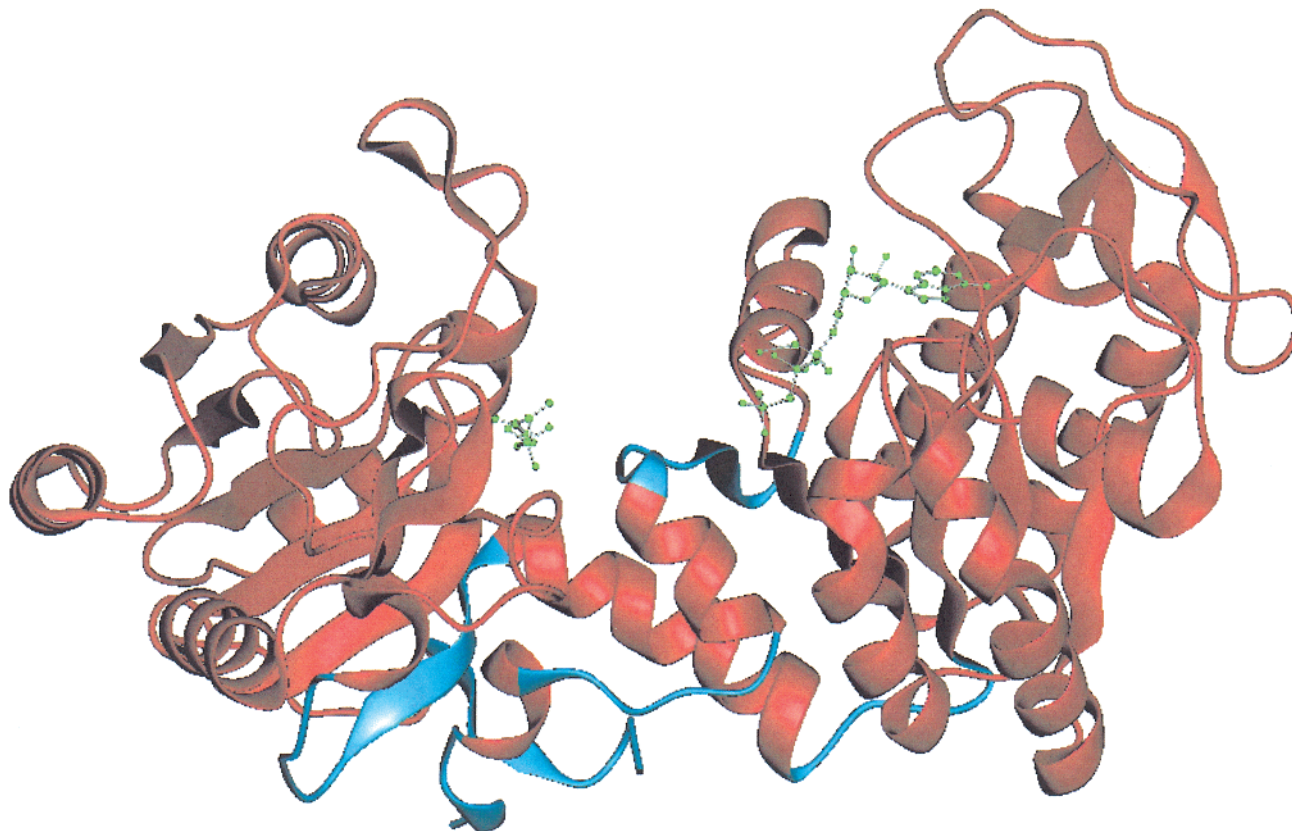


**Figure 1.** The H-NEIMO model for yeast R65Q PGK. The clusters or rigid bodies are shown in red while the movable residues are shown in cyan. The substrates are green. This is the  $C_{\alpha}$  trace of the model.

mechanism is plausible, although it does not rule out the possibility that the phosphoryl transfer may involve a second binding site for the 3-PG substrate. We also carried out normal all-atom MD dynamics (Cartesian MD) for comparison of the nature of domain rotations to H-NEIMO simulations. We find that the domains rotate about similar rotation axes for both the fine grain Cartesian MD and the coarse grain H-NEIMO MD. This demonstrates H-NEIMO MD as a fast mesoscale dynamics technique. Section 2 discusses the H-NEIMO algorithm and the simulation conditions. Section 3 contains the results and discussion from these simulations. Section 4 contains the simulation results and discussion from the simulations on trypanosomal *t.brucei* structure of PGK. Section 5 gives the conclusions.

## 2.0. Hierarchical NEIMO Algorithm

The Newton-Euler inverse mass operator method<sup>1</sup> (NEIMO) solves the constrained equations of motion efficiently by keeping all high frequency modes fixed. It also reduces the number of degrees of freedom from  $3N$  (where  $N$  is the number of atoms) to  $\mathcal{N}$  (the number of dihedral degrees of freedom) while allowing use of larger time steps than the Cartesian MD. For PGK,  $3N = 12525$  whereas  $\mathcal{N} = 2609$ . The equations of motion for constrained dynamics are

$$\ddot{\theta} = M^{-1}[T - C(\theta, \dot{\theta})] \quad (1)$$

Here  $\theta$  is the matrix of dihedral angles,  $M$  is the mass matrix for the clusters,  $T$  is the matrix of forces, and  $C$  is the velocity dependent Coriolis force.

The conventional algorithm<sup>14</sup> for solving constrained equations involves inverting the dense mass matrix  $M$  which scales as  $N^3$ , whereas NEIMO algorithm scales linearly with the

number of degrees of freedom. In the NEIMO algorithm the molecular system is partitioned into rigid bodies called “clusters” that are connected by “hinges” each of which can have one to six degrees of freedom. A cluster can consist of a single atom, a functional group such as C=O, or a phenyl ring, an  $\alpha$ -helix or even an entire domain of a protein. The hinge describes the relative motion between adjacent clusters. We have previously showed that NEIMO applied to proteins<sup>2</sup> and polymers<sup>3</sup> can give stable dynamics at time steps as high as 30fs. However, these studies considered polymers with random coil conformations. For large globular proteins, we find that residues far apart in sequence but in contact, can move close in a 30 fs time step, leading to bad contacts. Thus, we generally found time steps of 5–10 fs to be more reliable. The NEIMO algorithm has been combined with the massively parallel simulation (MPSim)<sup>15</sup> code which uses the cell multipole method<sup>16</sup> to calculate the nonbond interactions for very large systems on massively parallel computers. We have also extended<sup>3</sup> the NEIMO algorithm to perform Nosé-Hoover<sup>17,18</sup> constant temperature dynamics.

With NEIMO it is straightforward to build a hierarchy in which segments or parts of a domain of a molecule are clustered into rigid units while other sections in the same domain remain flexible. The NEIMO code has been automated to make terminal bonds and rings in a molecule as clusters. These are termed the “fundamental clusters”. In the H-NEIMO method the user could choose to combine these fundamental clusters into bigger clusters and allow the torsions connecting these bigger clusters as free hinges. Thus, a protein with two domains, for example, could be treated as two rigid bodies (the two domains) connected by torsions. To use all torsion NEIMO one could also model a protein as a collection of “fundamental clusters” (rings and

**TABLE 1: Time Steps Obtained in the Hierarchical Modeling of Two Large Proteins**

protein	MD method	degrees of freedom	time step(ps)
protein A <sup>a</sup>	Newtonian	1062	0.001
	NEIMO (all torsions)	219	0.010
	H-NEIMO	92	0.020
PGK	Newtonian (all atom)	12525	0.001
	NEIMO (all torsions)	2210	0.005
	H-NEIMO	80	0.010

<sup>a</sup> Protein A is a helix-coil-helix segment from staphylococcus aureus.

terminal bonds as clusters) connected by flexible torsions. H-NEIMO allows the user to choose several levels of granularity for the dynamics modeling of the molecular system. This kind of hierarchy allows the analysis of low-frequency dihedral motions between domains in PGK while keeping rigid most of each large domain. Also this method of coarse graining leads to larger time steps of integration in the MD. Table 1 shows the maximum possible time steps used for hierarchy of levels of MD simulations for 2 proteins. It is clear that fewer the number of degrees of freedom used larger the time step obtained for the coarse grain simulations. However, it should be remembered that the time steps obtained also depends on the granularity of the cluster model used for the H-NEIMO MD simulations. Similar to the NEIMO algorithm the H-NEIMO algorithm solves the constrained equations of motion recursively for each cluster as previously described in ref 3, for the NEIMO algorithm. We use the leapfrog Verlet algorithm to obtain velocities and coordinates from the accelerations.

Here we present constant temperature H-NEIMO simulations on yeast (R65Q) structure<sup>9</sup> and also the trypanosomal structure<sup>10</sup> of the ternary complex of PGK (referred to as *t.brucei* structure in this paper). Both these structures are ternary complexes of PGK, yeast R65Q in the open domain conformation and the *t.brucei* in the close domain conformation.

**2.1. Simulation Conditions.** The H-NEIMO-Hoover MD simulations were performed for 100 ps at temperature 300 and with time step 5 fs. We found that time steps of 10 fs generally led to stable dynamics for long times, but occasionally (about once every 10–50 ps) there would be a sharp change in the dynamics. This resulted because residues widely separated in the sequence but in close contact could occasionally lead to sufficiently larger coordinate increase to cause bad contacts. The relaxation time constant that determines Nosé mass factor was set to 10 times the time step in all the simulations.

Starting structures of *t.brucei*<sup>10</sup> (closed domain structure) and the yeast PGK<sup>9</sup> were taken from the Brookhaven protein databank. Counterions Na<sup>+</sup> and Cl<sup>-</sup> were added to neutralize the side chain charges on acidic and basic residues such as Asp, Glu, Arg, and Lys. The crystal structure of the ternary complex of R65Q mutant of yeast structure contains the substrates magnesium 5'-adenylylimidodiphosphate (Mg-AMP-PNP) and 3-phosphoglycerate (3PG). This structure has the open domain conformation with the substrates separated by ~13 Å leading to an interdomain cleft. Charges for the substrates were assigned using the charge equilibration method<sup>19</sup> with a net charge of -3e on 3PG and -2e on Mg-AMP-PNP. No counterions were placed near the residues Arg-38, Arg-121, and Lys-73 side chains since these residues coordinate with the carboxylate and phosphate of 3-PG. The  $\gamma$ -phosphate group of the Mg-AMP-PNP complex is favorably coordinated to Mg<sup>2+</sup> ion and the side chain of Lys-217. The resulting overall structure is neutral.

AMBER<sup>20</sup> force field (FF) was used for the protein and Mg-AMP-PNP and DREIDING FF<sup>21</sup> for the 3-PG. The nonbonds were treated using the Cell Multipole Method and a distance dependent dielectric used for implicit solvent shielding. Conjugate gradient minimization of the total energy was performed on the crystal structure until the overall RMS in force is <0.1kcal/mol/Å. The RMS deviation in coordinates (CRMS) of the minimized structure from the crystal structure is 0.684 Å, which is within the experimental resolution of the crystal structure (1.8 Å).

**Choice of H-NEIMO Clusters.** H-NEIMO-Hoover simulations were performed starting with the minimized structure at 300 K for 100 ps with time step of 5 fs. The dynamics was done on the yeast PGK structure using the MPSim code on Origin2000 supercomputer. We superimposed the centers of mass of the N and the C-domains of the yeast R65Q over the *t.brucei* PGK respectively and observed that the domain structures are preserved. Since our goal was to simulate the large scale domain motions going from the open to the closed form it was logical to treat major parts of the N and C domains of PGK as clusters during the dynamics. The cluster model used in the present simulation is shown in Figure 1. Parts of the yeast PGK shown in red in Figure 1 are kept rigid and the cyan torsions are flexible. The  $\phi$ ,  $\psi$  and the side chain torsion angles for the residues 1–8, 174–185, 198–205, 385–394, 400–406, and 409–415 were kept free during the H-NEIMO simulations. The torsion angles of the remaining residues were treated as fixed. The choice of clusters was based on the crystallographer's definition of the C and N-domain in PGK.<sup>9</sup> The helices in the inter-domain region were also kept rigid. This reduces the number of torsional degrees of freedom from 2210 to 80. The H-NEIMO model used for the *t.brucei* closed domain structure is described in section 4.1. The all atom Cartesian simulations were also performed for the yeast PGK using the Nosé-Hoover constant temperature method in MPSim code. The Cartesian simulation was performed at 300 K for 100 ps using 0.001 ps time step.

### 3.0. Results and Discussion

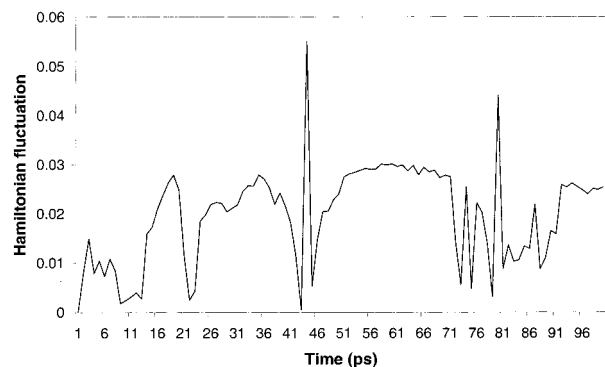
**3.1. CRMS and Fluctuations in Hamiltonian during H-NEIMO Dynamics.** The difference in RMS in coordinates (CRMS) for the C $_{\alpha}$  atoms in the N-domain between the crystal structure and the snapshots at different times during the dynamics were calculated. The CRMS values for these structures range between 0.01 and 1.3 Å. Likewise, the CRMS for the C $_{\alpha}$  atoms in the C-domain for various dynamics structures compared to the crystal structure is less than 1 Å. However, the overall CRMS for all the C $_{\alpha}$  atoms ranges from 2 to 5 Å. This is due to the large motion in the inter-domain region that pushes both the domains together. However, the CRMS for the N-domain is larger than the C-domain since the N-domain has parts that includes the flexible loop region. The loop between residues 173–184 that connects the N-domain to the interdomain region initiates a piston like motion that pushes the domains together.

Figure 2 shows the fluctuations in the Hamiltonian,  $\Delta H(t)$  at time  $t$  (ps) defined by

$$\Delta H(t) = \left| \frac{H(t) - H(0)}{H(0)} \right| \quad (2)$$

plotted as a function of time over the 100 ps of the H-NEIMO simulations of the yeast PGK. It can be seen that the average fluctuations in the Hamiltonian are of the order of  $10^{-2}$  that is





**Figure 2.** Absolute value of Hamiltonian fluctuation for yeast PGK, during the 100ps H-NEIMO simulations. This quantity is calculated using eq 2.

tolerable for use as a conformational search tool driven by real molecular forces. However, this may not be adequate for computing thermodynamic properties. Instead, we would use conformations extracted from the H-NEIMO dynamics for further fine grain Cartesian dynamics to calculate the thermodynamic properties. We found that the cumulative average of the Hamiltonian fluctuations reaches a plateau around fluctuation of  $10^{-2}$ .

**3.2. Analysis of Domain Motions in Yeast PGK and Comparison to *t.brucei* Structure.** During dynamics the two

domains of yeast PGK structure close and fluctuate around the closed domain conformation opening slightly but not completely. The closing of the domains is initiated with a piston like motion of the helix 7 initiated from the loop region (residue 173 to 184) in the N-domain. The domains undergo a rotation or a twist about the axes discussed in the next section. This rotation brings the two substrates AMP-PNP and 3PG together during the dynamics from 12.87 Å to 9.77 Å as seen in Figure 3. The variation of the distance between the centers of mass of the C- and N-domains in yeast PGK is shown in Figure 4. The trend in Figure 4 (a polynomial fit) again shows that the domains close and open during the H-ENIMO dynamics. Matching the centers of mass of the N and the C-domains of the various snapshots from the dynamics to the closed domain *t.brucei* structure shows that the CRMS for the C-domain ranges from 0.38 to 0.96 Å. The corresponding N-domains match with CRMS of 0.02–1.3 Å, while for the overall structure the CRMS is greater than 4 Å. Thus, during dynamics the domains remain intact in going from an open domain conformation to a closed domain conformation. The same is true in the crystal structures of R65Q yeast compared to the *t.brucei* structure. Motion in the interdomain region is mainly responsible for the large domain motions observed in yeast PGK.

For describing domain motions in PGK, crystallographers use the rotation axis between two experimental crystal structures.<sup>5,9–12</sup> This is the only pertaining experimental quantity available for

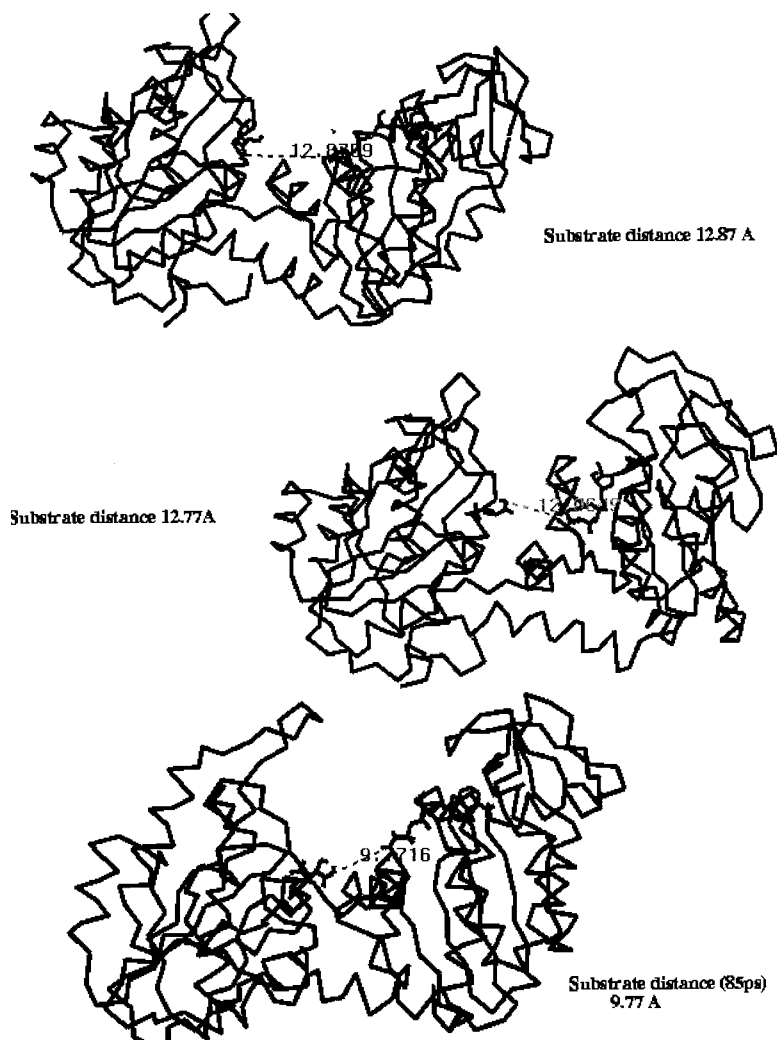


**Figure 3.** Three snapshots of R65Q yeast PGK at 0, 50, and 82.5 ps during H-NEIMO dynamics. The distance between the substrates (Phosphorus atom of  $\gamma$ - $\text{PO}_4$  group and the first carbon of 3-PG) to decrease with time.

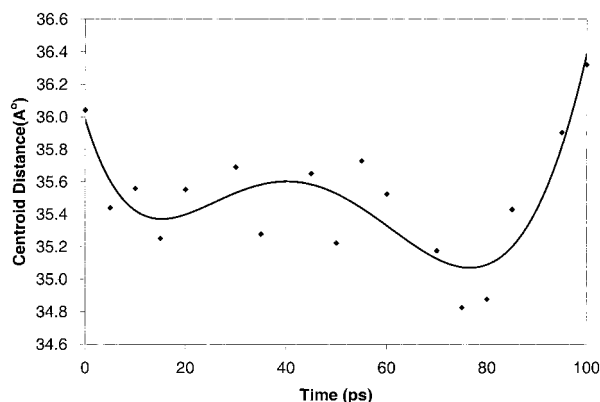


**Figure 4.** Variation of the distance between the center of mass of the N-domain and the C-domain in R65Q yeast PGK, with dynamics time in picoseconds. A polynomial fit is shown to reflect the trend in the variation.

comparison. We have made this comparison in this section. The relative orientations of the domains of PGK generated during the H-NEIMO MD dynamics to those of the starting structure yeast PGK have been calculated. The C-domain of H-NEIMO dynamics snapshot was superimposed on the C-domain of the yeast R65Q crystal structure. Following this the rigid body coordinate transformation that superimposes the N-domain of each of the structures on the N-domain of yeast R65Q structure was calculated. The three Euler angles thus obtained were transformed to spherical angles that define an axis of rotation and an angle of rotation about this axis. We also computed the same domain rotations for the experimental structures of yeast R65Q and *t.brucei* PGK. The matching of domains for nonidentical sequences were done in the conserved regions and regions of great structural similarity. Figure 5 shows the average

**TABLE 2: Angle of Rotations for Each Snapshot of Dynamics Structure Relative to the Starting Structure**

time (ps)	yeast R65Q PGK <sup>a</sup>	cartesian for yeast R65Q <sup>b</sup>	<i>t.brucei</i> PGK <sup>c</sup>
5.0	22.80	8.94	27.52
10.0	21.11	11.23	15.17
15.0	39.94	17.22	9.24
20.0	39.77	19.68	1.65
25.0	45.43	23.71	0.32
30.0	46.35	28.50	0.32
35.0	42.58	34.31	0.26
40.0	34.81	38.98	0.35
45.0	33.33	38.26	0.34
50.0	44.26	43.62	0.29
55.0	42.90	46.31	0.26
60.0	41.29	46.47	0.34
65.0	42.34	50.08	0.42
70.0	42.93	53.56	0.44
75.0	45.92	46.43	0.46
80.0	46.14	50.87	0.48
85.0	44.25	51.76	0.40
90.0	45.62	46.48	0.49
95.0	47.31	50.67	0.43
100.0	44.56	43.66	0.35

<sup>a</sup> Angle of domain rotation of H-NEIMO dynamics structures of yeast R65Q yeast PGK relative to the crystal structure of yeast R65Q PGK. <sup>b</sup> Angle of domain rotation for all atom Cartesian simulations on R65Q yeast relative to its crystal structure. <sup>c</sup> Angle of domain rotation for *t.brucei* PGK H-NEIMO structures relative to its crystal structure.

rotation axis for the H-NEIMO simulations compared to the *experimental rotation axis* in going from the open domain yeast PGK to the closed domain *t.brucei* structure. Although the rotation axis for H-NEIMO does not coincide with the one

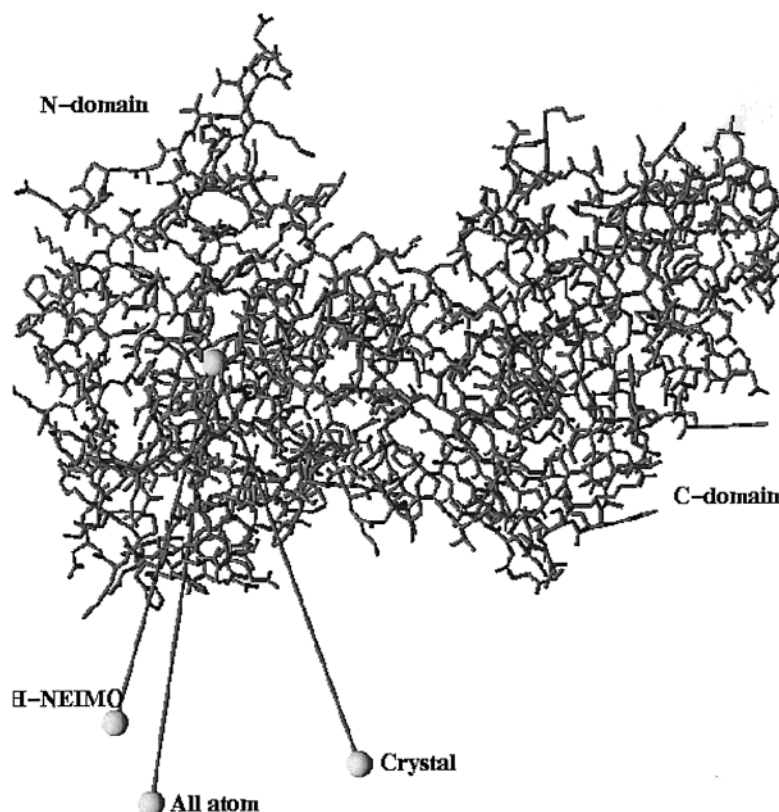


**Figure 5.** Axis labeled as H-NEIMO is the rotation axis calculated for superimposing the N-domains of the H-NEIMO structures of the R65Q yeast PGK with the crystal structure of R65Q yeast PGK. Label "Crystal" indicates the rotation axis calculated for superimposing the N-domain of yeast R65Q crystal structure with the *t.brucei* PGK crystal structure. Label "All atom" indicates the rotation axis for Cartesian all atom simulations.

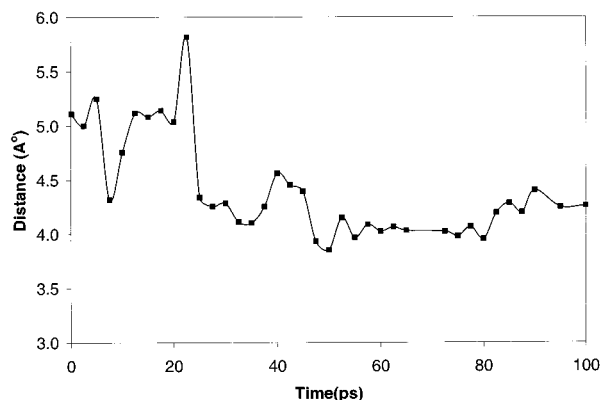


**Figure 6.** Variation of the distance between the phosphorus atom of  $\gamma$ - $\text{PO}_4$  of AMP-PNP and the  $\text{C}_\alpha$  atom of Gly371.

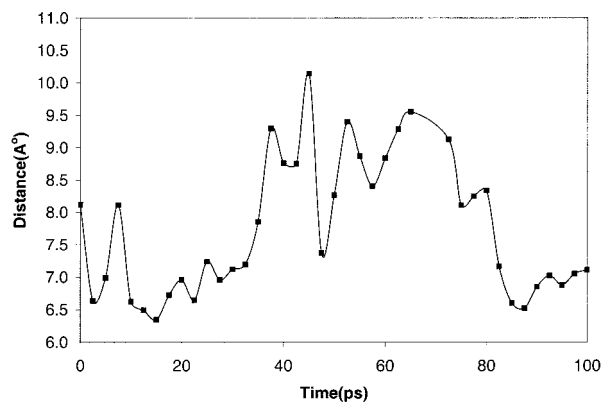


**Figure 7.** Variation of the distance between  $\gamma$ - $\text{PO}_4$  of AMP-PNP and  $\text{C}_\alpha$  of Gly-394 during the H-NEIMO dynamics of yeast PGK.

for crystal structures they are in the same region of the N-domain. Bernstein et al.<sup>10</sup> have calculated the angle of rotation in going from horse PGK (open domain) to *t.brucei* PGK as  $32^\circ$ . This compares well with the  $32.93^\circ$  angle of rotation that we have calculated for the yeast structure to be superimposed on *t.brucei* structure. The second column of Table 2 shows the distribution of rotation angles for various snapshots during the dynamics starting with the yeast R65Q PGK structure. The rotation angle varies from  $21^\circ$  to  $46^\circ$  fluctuating around  $40^\circ$ . The snapshot at 45ps of H-NEIMO dynamics of yeast PGK has an angle of rotation  $33.33^\circ$ . This is close to the experimental angle of rotation between yeast and *t.brucei* PGK. Since the sequences of *t.brucei* and the yeast R65Q PGK are different, it is incorrect to expect to reproduce the closed domain structure of *t.brucei* structure from the dynamics of the R65Q structure. However, as discussed before the domain structures of PGK during dynamics and that of *t.brucei* crystal structure agree well. Thus, the dynamics elucidates the nature of domain motion and gives insight into the possible conformations and active sites in PGK as discussed in the next section.

**3.3. Possible Involvement of Helix 14 in the Mechanism of Phosphoryl Transfer.** It has been speculated<sup>9</sup> that both helix 13 and helix-14 (residues 371 to 380 and 394 to 401 in the yeast structure) are involved in the catalytic process of phosphoryl transfer. Bernstein et al.<sup>10</sup> modeled a phosphate group that is to be transferred, bound to the Gly-394 (Gly-399 in the *t.brucei* structure). We indeed find during the dynamics that the  $\gamma$  phosphate of AMP-PNP flips and moves closer to the Gly-371 and Gly-394. Figure 6 shows the variation of the distance between the phosphorus atom of  $\gamma$ -phosphate of AMP-PNP and the  $\text{C}_\alpha$  atom of Gly-371 in the yeast PGK structure. This distance decreases to 4 Å and fluctuates around

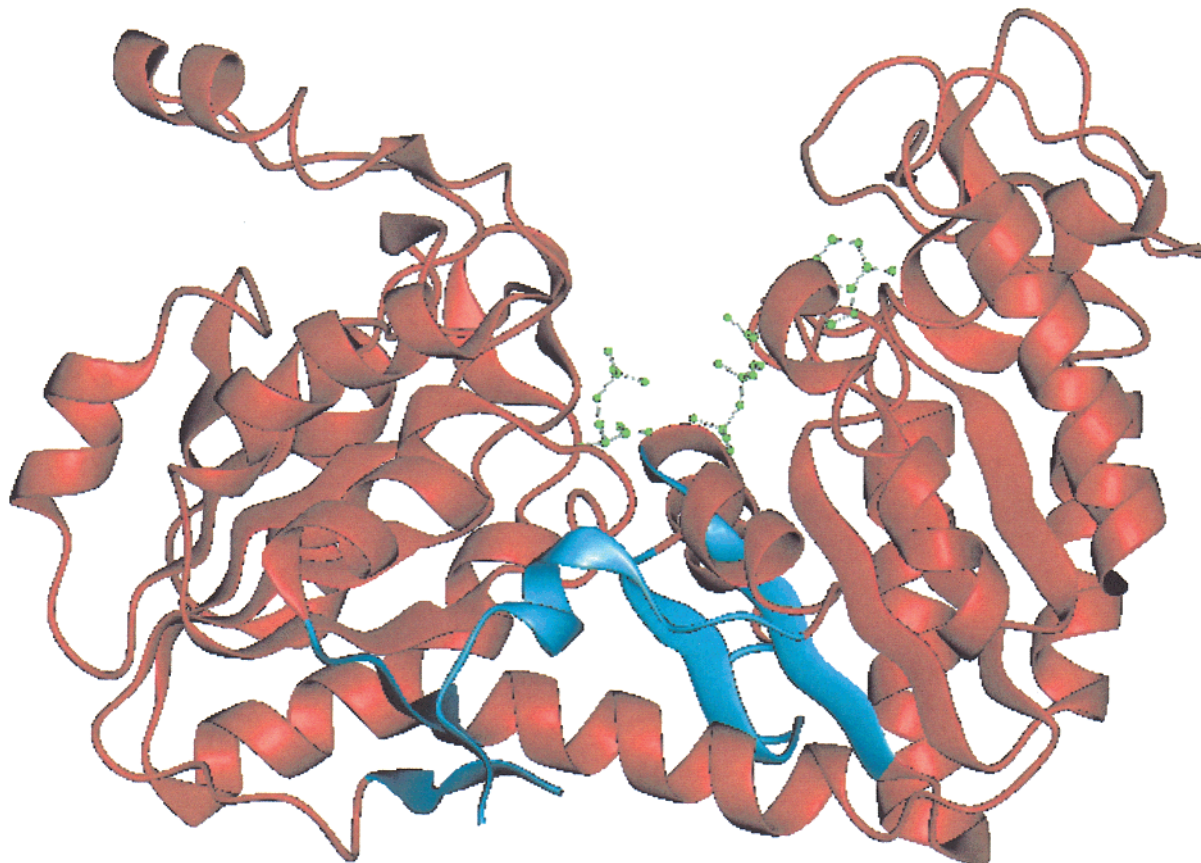


**Figure 8.** H-NEIMO cluster model for *t.brucei* PGK. The rigid bodies are shown in red and movable residues in cyan. The ranges of the residues are listed in the text.

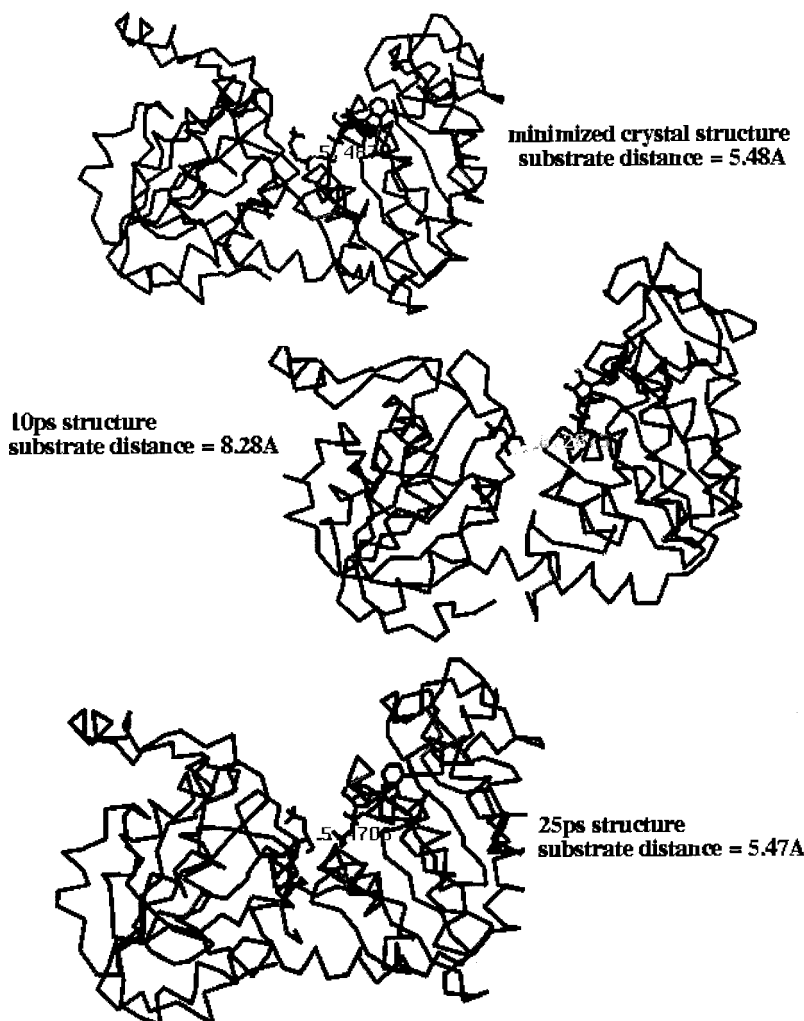


**Figure 9.** Snapshots of *t.brucei* PGK at 0, 10, and 25 ps during H-NEIMO dynamics. This shows the domains do not open up during the H-NEIMO simulations starting from a closed domain *t.brucei* structure.

this value subsequently, as speculated. Figure 7 shows the distance between the phosphorus atom of  $\gamma$ -phosphate of AMP-PNP and the  $C_{\alpha}$  atom of Gly-394. This distance fluctuates between 6.3 Å and 10 Å, thus creating the possibility of coordination of the transferable  $PO_4$  docked on Gly-394 to the ADP during the reaction. Bernstein et al. also suggested that the phosphate of 3-PG could coordinate with the Gly-394 but we find that this distance increases during the dynamics making this interaction less likely.

**3.4. Comparison of Coarse Grain H-NEIMO Dynamics to Fine Grain Cartesian MD.** To understand the domain space spanned by coarse grain H-NEIMO MD as compared to the fine grain Cartesian MD we have compared the domain rotations in these two simulations. Cartesian simulations were performed on the open domain yeast R65Q PGK structure with 1 fs time step at 300 K with the same FF and under the same conditions as the H-NEIMO simulations. The same starting structure (crystal structure minimized) has been used in the Cartesian simulations. Here the total number of degrees of freedom is 12525. The domain rotations in the Cartesian simulations have been analyzed as described in the previous section. Column 3 of Table 2 shows the rotation angles for the domain rotations. These vary from 0 to 55° that are in the same range as the H-NEIMO simulations. It is seen from Figure 5 that the average rotation axis for domain rotations for the Cartesian simulations is close to that of H-NEIMO dynamics. This is a good proof that the H-NEIMO MD dynamics searches a subspace of the

Cartesian space in a much more time efficient fashion. Hence H-NEIMO could be used to study large scale time motions in proteins much faster than all atom MD simulations.

To be able to study large scale domain motions in proteins using H-NEIMO, one needs to know the residues that are in the domains and the torsions that are likely to initiate the domain motions. However, given the crystal structure of the protein the domain and the interdomain regions can be easily identified. Other choices of clusters would lead to the same domain motions but in a much longer time scale. Focusing the dynamics on the torsions in the interdomain region exhibits large scale motions in a short computational time. H-NEIMO method is nevertheless a MD method and hence cannot be used presently for folding a large protein starting from its sequence. But, the kinetics of folding of polypeptides has been studied<sup>4</sup> using NEIMO method. This paper demonstrates the use of the H-NEIMO method as a conformational search tool driven by real forces when the structural changes are within 5 to 7 Å. H-NEIMO method can be used with any level description of the solvent, namely explicit solvent simulations, or Poisson-Boltzmann<sup>22</sup> description of solvation or implicit solvent description. In this paper we used the distance dependent dielectric description for the solvent. Including explicit solvent in the simulations would lead to a great increase in the fluctuations for the domain dynamics, thus increasing the time scale to observe the large scale domain motions.



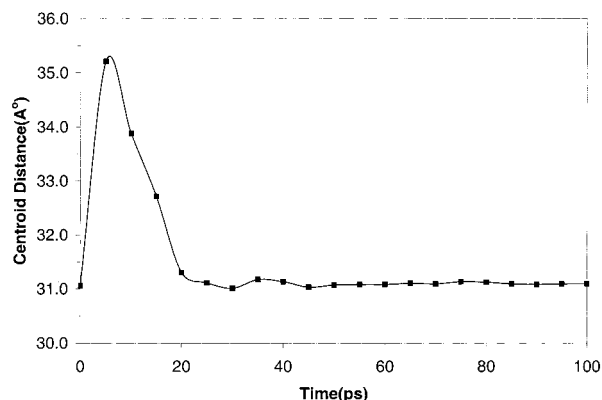


**Figure 10.** Variation of the distance between the centers of mass of N and C-domains of *t.brucei* PGK during the H-NEIMO dynamics.

#### 4.0. H-NEIMO Dynamics on the Trypanosoma PGK

The crystal structure trypanosoma PGK is the first ternary complex crystallized in a closed conformation. In this structure the N and the C-domains of PGK are closed and the substrates ADP and 3-PG are  $\sim 5$  Å apart. The substrates in this crystal structure are a combination of product (3-PG) and reactant (ADP). To examine if we could open up the close domain structure of PGK we performed the H-NEIMO simulations on *t.brucei* PGK. The *t.brucei* structure has slightly different sequence than the yeast R65Q PGK. Most of the sequence differences are in the loop regions. Counterions,  $\text{Na}^+$  and  $\text{Cl}^-$ , were added to neutralize the acidic and basic residues except for those that form salt bridges. The AMBER FF for the protein and ADP and DREIDING FF was used for the 3-PG substrates. Charges were assigned to 3PG and Mg-ADP using charge equilibration method with a net charge of  $-3e$  and  $-1e$  on 3PG and Mg-ADP, respectively. The structure was then minimized to an overall RMS in force of  $0.1$  kcal/mol/Å. The CRMS of the minimized structure from the crystal structure is  $1.12$  Å, well within the resolution of crystal structure of  $2.8$  Å.

**4.1. H-NEIMO Dynamics on the *t.brucei* structure.** The choice of clusters and hinges for H-NEIMO model of the *t.brucei* PGK was also based on the crystallographer's definition of the N and C domains. The helices in the inter-domain region were also treated as clusters. The clustering model used *t.brucei* structure is shown in Figure 8, the clusters shown in red and the hinges in cyan. Residues 8–184, 191–369, 376–386, and 397–406 were defined as clusters, and torsion angles of remaining residues were allowed to move during the simulations. Constant temperature H-NEIMO dynamics was performed for 100 ps on one node of Origin2000 supercomputer using time step 0.005 ps at 300 K. The relaxation time related to Nosé mass factor was set to 10 times the time step.

**4.2. Results of H-NEIMO Dynamics.** During the dynamics, the structure opens up in the first 25 ps and then the domains close to the starting structure as shown in Figure 9. The overall CRMS difference between the starting structure and the H-NEIMO dynamics structures after 25 ps are within  $1.2$  Å. The average CRMS variation for the N-domain during the dynamics is  $0.47$  Å and for the C-domain is  $0.57$  Å. Figure 10 shows the variation of the distance between the substrates ADP and 3-PG with time. These distances were measured from the phosphorus atom of the  $\beta$  phosphate group of ADP and the first carbon of the 3-PG substrate. At first this distance increases as the domains open up and then decreases back to around  $7.2$  Å. While the dynamics of yeast PGK shows large domain motions, the dynamics of the *t.brucei* structure does not show motions of

the same scale. This may be because when two substrates are bound the closed conformation is more stable for the protein than the open conformation. It is also possible that there is an activation barrier to go from the  $9$  Å close domain structure obtained from the H-NEIMO dynamics on yeast PGK to the close domain *t.brucei* structure.

#### 4.3. Analysis of Domain Motion in *T.brucei* Structure.

C-domains of various H-NEIMO dynamics snapshots were superimposed on the C-domain of the *t.brucei* crystal structure. The rigid body rotations required to further superimpose the corresponding N-domains were calculated. The fourth column of Table 2 shows the angle of rotation for superimposing the structures. The angle increases in the initial period of dynamics and then decreases close to  $0.0^\circ$  after 25 ps. In the case of yeast PGK the dynamics closed the domains and the rotation angles are distributed around  $35^\circ$  after closing up the domains. In the *t.brucei* structure the domains opened up slightly and then closed back to the original positions. This shows that the closed domain structure could be more stable for the protein when both the substrates are bound.

#### 5.0. Conclusions

Using the hierarchical NEIMO methodology, we have been able to study the long time scale domain motions in PGK. H-NEIMO allows us to focus on the inter-domain torsional angles responsible for the long-time scale domain motions. This allowed us to study the inter-domain motions in fairly short simulation time scale (100 ps) [much faster than the actual time scale for these motions, which are slowed by frictional effects due to the high-frequency modes).

We see that residues 175–183 initiates a piston like motion on the helix 7 in the inter-domain region which causes a push upward to the C-domain. Gly-394 of the yeast structure is possibly involved in the catalysis process as shown during the simulations. Thus it is possible that the  $\gamma$ -phosphate of AMP-PNP substrate would coordinate to the Gly-394 of yeast structure and the oxygen of the carboxylate of 3PG which picks up the  $\gamma$ -phosphate from AMP-PNP.

This demonstrates that H-NEIMO can be used as a coarse grain mesoscale MD technique for studying long time scale motions. The domain rotations generated during the H-NEIMO correspond well to those of experimental structures and Cartesian simulations.

**Acknowledgment.** The authors thank Dr. Timothy McPhillips of the Stanford Synchrotron Research Laboratory for his significant help in carrying out this research, with many useful discussions. This research was funded by NSF-SGER-DBI-9708929 (Dr. Karl Koehler). The computational resources in the MSC used in this work were supported by grants from NSF-GCAG, NSF-CHEM, ARO-DARPA, ARO-MURI (Kisero), by Beckman Institute, BP Amoco, Chevron Corp, Exxon, Seiko-Epson, Owens-Corning, Avery-Dennison, Dow Chemical, and 3M.

#### References and Notes

- (1) Jain, A.; Vaidehi, N.; Rodriguez, G. *J. Comput. Phys.* **1993**, *106*, 258.
- (2) A.Mathiowetz, A. M. Jain, A., Karasawa, N., and Goddard, W. A., III *Proteins: Struct., Funct. and Genet.* **1994**, *20*, 227.
- (3) Vaidehi, N.; Jain A.; Goddard, W. A., III *J. Phys. Chem.* **1996**, *100*, 10508.



- (4) Bertsch, R. A.; Vaidehi, N.; Chan, S. I.; Goddard, W. A., III *Proteins: Struct., Funct., Genet.* **1998**, *33*, 1.
- (5) Blake, C. C. F.; Evans, P. R. *J. Mol. Biol.* **1974**, *84*, 585.
- (6) Watson, H. C.; Walker, N. P. C.; Shaw, P. J.; Bryant, T. N.; Wendell, P. L.; Fothergill, R. L.; Perkins, R. E.; Conroy, S. C.; Dobson, M. J.; Tuite, M. F.; Kingsman, A. J.; Kingsman, S. M. *EMBO J.* **1982**, *1*, 1635.
- (7) Davies, G. J.; Gamblin, S. J.; Littlechild J. A.; Watson, H. C. *Acta Crystallogr.* **1994**, *D50*, 202.
- (8) Harlos, K.; Vas M.; Blake, C. F. *Proteins: Struct., Funct., Genet.* **1992**, *12*, 133.
- (9) McPhillips, T. M.; Hsu, B. T.; Sherman, M. A.; Mas, M. T.; Rees, D. C. *Biochemistry* **1996**, *35*, 4118.
- (10) Bernstein, B. E.; Michels, P. A. M.; Hol, W. G. J. *Nature* **1997**, *385*, 275.
- (11) Bernstein, B. E.; Williams, D. M.; Bressi, J. C.; Kuhn, P.; Gelb, M. H.; Blackburn, G. M.; Hol, Wm. G. *J. Mol. Biol.*, **1998**, *279*, 1137.
- (12) Auerbach, G.; Huber, R.; Grattinger M.; Zaiss, K.; Schurig, H.; Jaenicke, R.; Jacob, U. *Structure*, **1997**, *5*, 1475.
- (13) Banks, R. D.; Blake, C. C. F.; Evans, P. R.; Haser, R.; Rice, D. W.; Hardy, G. W.; Merett, M.; Phillips, A. W. *Nature* **1979**, *279*, 773.
- (14) Mazur, A.; Abagayan, R. *J. Biomol. Struct. Dyn.* **1989**, *6*, 815.
- (15) Lim, K. T.; Brunett, S.; Iotov, M.; McClurg, B.; Vaidehi, N.; Dasgupta, S.; Taylor, S.; Goddard, W. A., III *J. Comput. Chem.* **1997**, *18*, 501.
- (16) Ding, H. Q.; Karasawa, N.; Goddard, W. A., III *J. Chem. Phys.* **1992**, *97*, 4309.
- (17) Nosé, S. *J. Chem. Phys.* **1984**, *81*, 511.
- (18) Hoover, W. G. *Phys. Rev.* **1985**, *A31*, 1695.
- (19) Weiner, S. J.; Kollman, P. A.; Case, D. A.; Singh, U. C.; Gio, C.; Alagona, G.; Profeta, S., Jr.; Weiner, P. *J. Am. Chem. Soc.* **1984**, *106*, 765.
- (20) Mayo, S.; Olafson, B. D.; Goddard, W. A., III *J. Phys. Chem.* **1990**, *94*, 8897.
- (21) Rappé A.; Goddard, W. A., III *J. Phys. Chem.* **1991**, *95*, 3358.
- (22) Tannor, D. J.; Marten, B.; Murphy, R.; Friesner, R. A.; Sitkoff, D.; Nocholls, A.; Ringnalda, M. N.; Goddard, W. A., III; Honig, B. *J. Am. Chem. Soc.* **1994**, *116*, 11875.